Letter to the Editor

Discovery of a new gravitationally lensed QSO with broad absorption lines*

L. Wisotzki, T. Köhler, S. Lopez, and D. Reimers

Hamburger Sternwarte, Gojenbergsweg 112, D-21029 Hamburg, Germany (lwisotzki@hs.uni-hamburg.de)

Received 16 July 1996 / Accepted 20 August 1996

Abstract. We announce the discovery of a new bright gravitionally lensed QSO, HE 2149-2745. The object, at z=2.033, presents two images separated by 1"7, with B magnitudes 17.3 and 19.0, respectively. Their spectra look identical within the measurement errors; in particular, both components display indistinguishable P Cygnitype emission/absorption complexes. Near to the line of sight to the brighter component, an extended source with $R \simeq 19.8$ is detected which could be responsible for the lensing. If it is a luminous galaxy $(L \simeq L^*)$, we infer a probable redshift range of ~ 0.2 -0.5.

Key words: Quasars: indidual: HE 2149-2745-Quasars: general - Gravitational lensing

1. Introduction

Since 1990 we conduct a wide-angle survey for bright QSOs (the Hamburg/ESO survey; HES), intended to sample the quasar population with $B \lesssim 17.5$ and $z \lesssim 3.2$ over a substantial fraction of the southern extragalactic sky (Wisotzki et al. 1996; Reimers et al. 1996). One of the prime scientific aims of this project is the discovery of new gravitationally lensed QSOs. Since high-luminosity quasars appear to have a higher a-priori probability of being lensed (e.g., Surdej et al. 1993), our survey should be particularly well suited for such a task.

A first successful finding was the bright double QSO HE 1104–1805 (the 'Double Hamburger'; Wisotzki et al. 1993) which is most probably a gravitational mirage (cf. also Wisotzki et al. 1995 and Smette et al. 1995). Here we report about another QSO discovered in the course of the HES, recently identified as gravitationally lensed binary image.

Send offprint requests to: L. Wisotzki

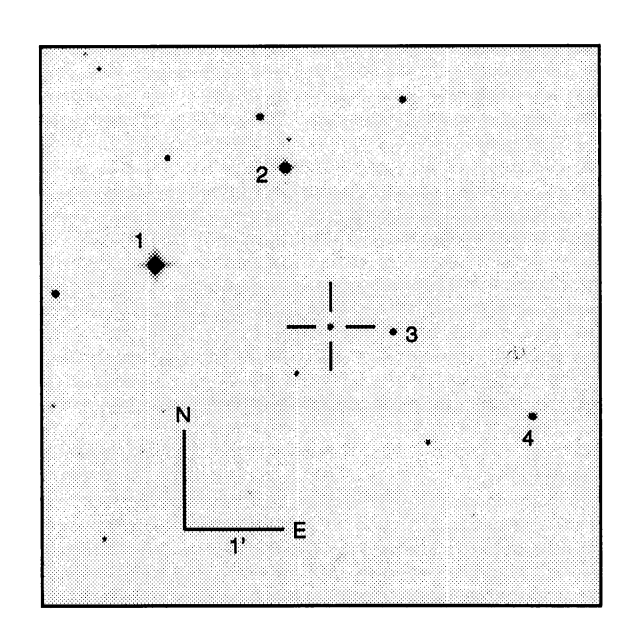


Fig. 1. Finding chart for the double QSO HE 2149-2745, from a B band CCD image taken with the ESO/MPI 2.2 m telescope. The coordinates of component A are: $\alpha = 21^{\rm h} \ 52^{\rm m} \ 07^{\rm s}.4$, $\delta = -27^{\rm o} \ 31' \ 50'' \ (\rm J2000.0)$. The stars marked by numbers 1-4 are referred to in the text.

2. Observations

HE 2149–2745 was discovered as quasar candidate on a digitised objective prism plate in the course of the Hamburg / ESO survey, because of its unusual continuum shape and a sharp spectral break in the UV. The target was observed during a regular candidate follow-up spectroscopic run in November 1994, using the ESO 1.52m telescope with its Boller & Chivens spectrograph. The discovery spectrum conspicuously showed already the broad absorption troughs characteristic of BAL QSOs, at a redshift of z=2.03. A few nights later we reobserved the same source at the ESO 3.6m telescope, now using EFOSC1

^{*} Based on observations made at the European Southern Observatory, La Silla, Chile



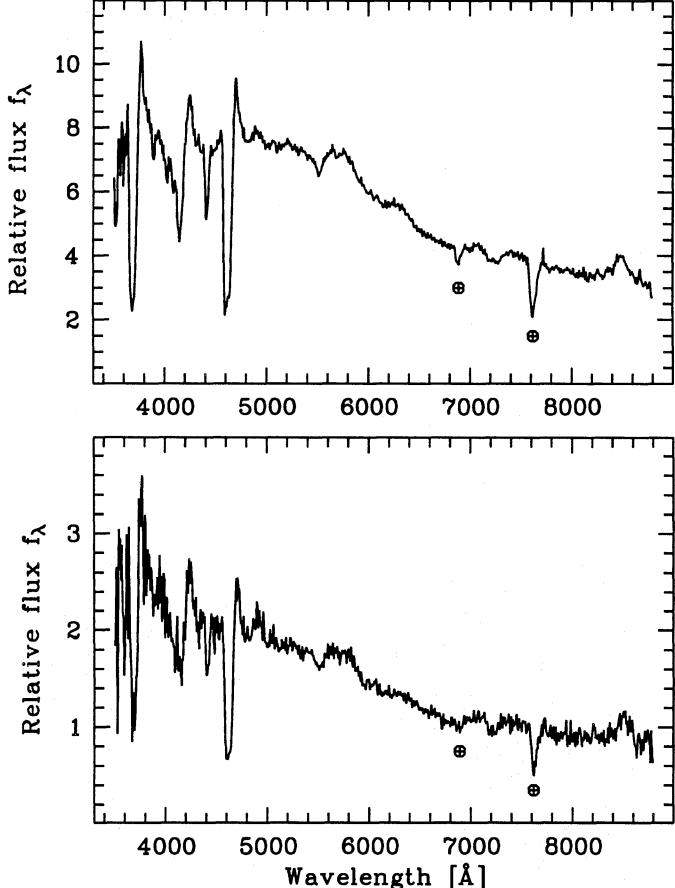


Fig. 2. Deblended low-resolution spectra of HE 2149-2745 A (top) and B (bottom). The symbols \oplus denote telluric absorption lines.

with its B150 grism, allowing for a higher spectral resolution of ~ 10 Å FWHM. This spectrum is displayed in Fig. 3. At the same occasion, we also obtained a direct image in which, upon close examination, the QSO showed some elongation. Because of mediocre seeing conditions, the poor detector sampling (0".6 per pixel) and the very high airmass already at the beginning of the night, we decided to postpone the investigation of the case to the following year.

New observations of this object were conducted on Oct 20th, 1995, with the ESO/MPI 2.2 m telescope, equipped with EFOSC2 and a Thomson 1k×1k CCD detector; the pixel size was 0".33. Bessel B and R band images obtained at $\sim 1''$ seeing allowed to resolve the QSO into two discrete point sources separated by 1".7 (cf. Fig. 4a). A 30 min exposure long-slit spectrum with the slit rotated at the position angle of 32° established that both sources showed the same peculiar BAL spectrum. Unfortunately, the seeing conditions deteriorated during that exposure to an effective FWHM of ~ 1.4 , but although the two point source profiles show considerable overlap, there can be no doubt that the same broad absorption lines are present in both

objects. The spectral resolution of these data, given by the size of the seeing disk within the slit, was about 35 Å (FWHM).

Despite the time-variable seeing, photometric transparency seemed to be reasonably stable during the night, and we observed several photometric (from Landolt 1992) as well as spectrophotometric (from the HST collation) standard stars for flux calibration purposes.

3. Analysis

$3.1. \ Photometry$

After bias subtraction and flat-fielding with twilight sky flats, the 2.2 m EFOSC2 direct images were fed into the DAOPHOT II package as implemented in ESO-MIDAS. Simple aperture photometry gave the total magnitude of HE 2149-2745 to $B_{A+B} = 17.11 \pm 0.06$ and $R_{A+B} =$ 16.26 ± 0.04 . The error estimates include the usual contributions such as readout and photon shot noise, as well as the zero-point uncertainty determined from several standard stars. Note that the given B magnitudes are reduced to the Bessel system, based on the measured B-R colour. The nearby star (marked '3' in Fig. 1) has B = 16.84 and R = 15.07.

Only very few stars in the field were suited to define the point-spread function (PSF), which is somewhat unfortunate in view of the spatial variations of the PSF over the field. Acceptable results were obtained by adopting a Moffat (1969) function with parameter $\beta = 2.5$ for the analytical PSF representation; resulting rms residuals of profile fits to single stars were then always less than $\sim 0.3\%$ of the count rate, approximately equal to the error tolerated by the flatfield. Simultaneous fits to the two QSO components yielded $B_A = 17.33$, $B_B = 18.95$ (magnitude difference $\Delta B_{A-B} = 1.62$), and $R_A = 16.49$, $R_B = 18.06$ (magnitude difference $\Delta R_{A-B} = 1.57$), respectively. The corresponding colours of the two images are $(B - R)_A = 0.84$ and $(B - R)_B = 0.89$, quite canonical values. However, the PSF fit to the QSO left considerably higher residuals than for isolated stars. We examine below the possibility that these residuals may be related to the superposition of a faint galaxy.

3.2. Astrometry

Three of the surrounding stars, marked in Fig. 1 by numbers 1, 2, and 4, are listed in the HST Guide Star Catalogue (GSC). Using the source centroids measured by DAOPHOT, we constructed a linear plate solution to obtain an accurate (J2000.0) position for the QSO. The coordinates of component A are $\alpha_A = 21^h 52^m 07.44$, $\delta_{\rm A} = -27^{\circ} \, 31' \, 50'' \, 2$; the coordinates of component B are $\alpha_{\rm B} = 21^{\rm h} 52^{\rm m} 07^{\rm s}.68$, $\delta_{\rm B} = -27^{\rm o} 31' 48''.7$. The internal error of these coordinates should be smaller than 0".1. The angular separation of the components is 1.70 ± 0.05 , the position angle is $32^{\circ} \pm 3^{\circ}$.

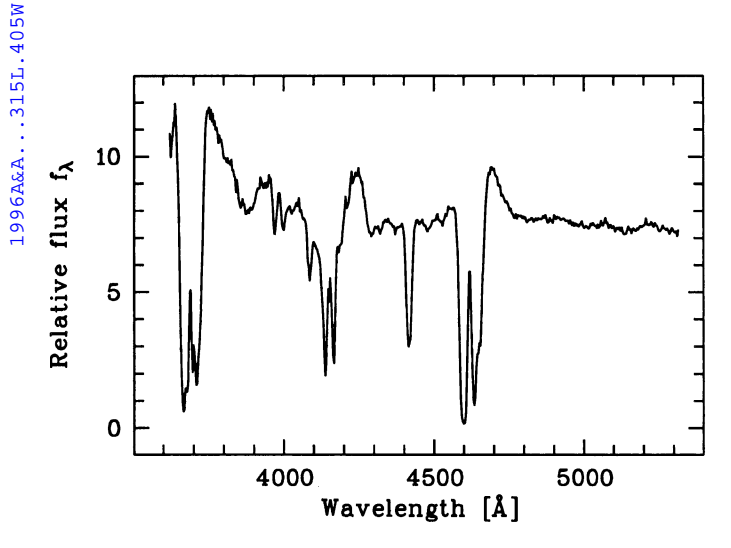


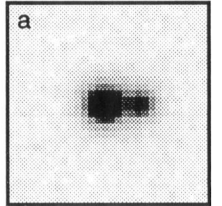
Fig. 3. 10 Å resolution spectrum of HE 2149-2745 A+B.

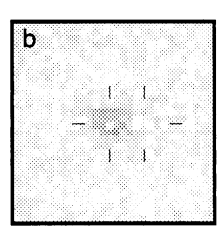
3.3. Spectroscopic properties

Although the double BAL-QSO nature of HE 2149–2745 was hardly in question, an important task was to decompose the badly blended long-slit spectrum as accurately as possible, to pursue the key question for gravitational lensing of QSOs: Do the components show, within measurement errors, identical spectra? If not, the case for lensing is generally much weaker though some sorts of differences can be allowed for. However, for objects with large brightness differences, blending can lead to a strong bias in favour of the brighter component when actually extracting the spectra. In our EFOSC2 data, additional complications were contributed by the spectrograph in form of a somewhat asymmetric PSF, and of chromatic variations of the PSF width particularly at $\lambda < 4500\,\text{Å}$.

The spectral frame was first reduced with standard procedures. We then proceeded with the algorithm used already by Smette et al. (1995), consisting of the following essential steps: (1) Two Gaussians, of the same FWHM and with fixed angular separation but otherwise unconstrained, were fitted simultaneously to each spectral resolution element. (2) The variation with wavelength of the resulting parameters FWHM and centroid location was fitted by low-order polynomials. (3) Another double-Gaussian fit was performed, now with only the two amplitudes as free parameters. The resulting wavelength and flux calibrated spectra are shown in Fig. 2. The emission redshift, determined from the peak position of Mg II at 8490 Å, is $z = 2.033 \pm 0.005$ for both objects.

The resemblance between the two spectra is striking. In particular, all the absorption lines are of equal strength – within the measurement accuracy – in both spectra. The steep wings of the broad absorption troughs, much more sensitive to small shifts in wavelength than normal QSO emission lines, coincide better than 100 km/s. The quotient of both spectra shows neither traces of emission nor of absorption lines, and the flux ratio, evaluated around





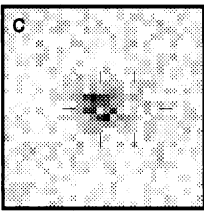


Fig. 4. Gray-scale images of the double QSO and the candidate lensing galaxy. Image size is 10", the orientation has been aligned to a position angle of 32°. a: QSO image; b: scaled point-spread function subtracted, same gray scale coding as image a; c: as before, but gray scale adjusted. The positions of QSO components A and B are marked.

6000 Å, is consistent with the value of 4.3 found from the photometry. We are thus confident that the extraction procedure has performed a reasonably unbiased deblending. For $\lambda < 4500$ Å, the flux ratio appears to decrease, visible as a steepening in the continuum slope of component B in Fig. 2. However, this is probably an artefact introduced by the strong degradation of the PSF width in the spectrograph, since the more reliable B-R colours do not confirm this trend. We therefore conclude that no significant differences between the spectra can be detected.

The blue part of the spectrum displays conspicuous P Cygni profiles of several high-ionisation lines, such as C IV $\lambda 1549$, Si IV $\lambda 1398$, and N V $\lambda 1240$ (cf. Fig. 3). The Ly α emission line seems to be almost completely absorbed by the N V BAL, not uncommon for this type of QSO. The most prominent absorption systems are blueshifted with respect to the expected emission line positions by velocities of ~ 1400 , ~ 2300 , and $\sim 19\,000$ km/s in the QSO rest frame. Note, however, that the line-to-line dispersion in velocity shift is several hundred km/s, without any discernible dependency on ionisation potential. These systems are probably also present in Al III $\lambda 1857$ (only low-resolution spectrum, Fig. 2). There is no indication of a BAL associated with Mg II $\lambda 2798$, but the S/N ratio is low in this part of the spectrum.

An interesting feature is the slight detachment of emission and absorption in the Si IV/O IV] $\lambda1400$ complex. The emission peaks at $\lambda_{\rm rest}=1401\,\rm \mathring{A}$, which is at a longer wavelength than usually found (e.g., Tytler & Fan 1992). It almost matches the position of O IV] $\lambda1402$ which is expected to occur in emission only, while the Si IV $\lambda1398$ emission line presumably suffers from absorption and is suppressed below its normal contribution.

As the 10 Å resolution spectrum seems to contain many more yet unresolved lines and line complexes, higher resolved spectroscopy will likely yield further identifications.

3.4. A candidate for the lensing galaxy

We stated above that the PSF fit to the R band direct image of HE 2149-2745 was not really satisfactory. After

subtracting the fitted profiles from the original frame, a visual inspection of the residual image prompted us to suspect a faint third, slightly extended component at more or less the location of QSO component A. While the profile was overfitted in the peak, leading to a negative central residual, the surrounding pixels were significantly positive, with a total count rate of 3% of that of the QSO.

We then manually reduced the PSF scaling factor of component A by 0.03 mag, so that no pixels contained significantly negative residuals (however, the central pixel still goes down to zero, so the approach was rather conservative). The resulting residual image is displayed in Fig. 4. An extended source of total magnitude R = 19.8 emerged, with a FWHM twice that of the point sources in the field. A plausible – though not the only possible – interpretation would be that we have detected the galaxy in the line of sight to the QSO which is responsible for the lensing. Note that inferred magnitude and position are based on a short exposure frame, and therefore still preliminary and quite uncertain. Much better data are required to confirm this detection, to improve on the decomposition method, and eventually to determine the intrinsic parameters of this galaxy.

We finally note that, to a magnitude limit of $R \simeq 22$, no other galaxies are visible close to the QSO, and that there is no evidence for a cluster within a radius of ~ 2.5 .

4. Conclusions

The similarity of spectral properties between the two components of HE 2149-2745 is so striking, even in detail, that we do not hesitate to invoke image splitting by gravitational lensing as the most probable explanation. This is then the third known instance of a gravitationally lensed QSO with broad absorption lines, after the 'clover leaf' H 1413+117 (Magain et al. 1988), and UM 425 (Michalitsianos & Oliversen 1995).

The detection of a galaxy in the line of sight fits well into the lens scenario. The measured magnitude is such that a galaxy redshift measurement is not out of the question, either with large ground-based telescopes under very good seeing conditions, or with HST. We can perform an order-of-magnitude estimate of the redshift if we assume that the lensing galaxy should be among the most massive of the normal galaxy population. Adopting $M_R \simeq -22$ (close to M^* for $H_0 = 50$ km s⁻¹ Mpc⁻¹ and $q_0 = 0.5$), we obtain a putative redshift of $z \simeq 0.35$, ignoring K corrections. Considering the uncertainties, we predict that the redshift is probably in the range $0.2 \lesssim z \lesssim 0.5$.

Since our discovery data are not of very high quality, better observational material is certainly required to proceed, in particular deep images obtained under good seeing conditions. Note that our data allow us to exclude that the residuals are *exclusively* due to a third point source which is expected for a simple symmetric lens; if additionally a

fourth, or even a fifth image is invoked, the constraints are, of course, much weaker.

HE 2149-2745 could be a new target to determine the time delay for intrinsic variability. A value of Δt of a few months can be expected, depending however sensitively on the relative deflector position. No variability information is yet available, thus a regular photometric monitoring of this interesting new system should be installed soon.

Acknowledgements. We thank R. Kayser for an informative discussion, and the referee for helpful comments. T.K. acknowledges support from the DFG under grants Re 353/33-1 and -2.

References

Landolt A.U., 1992, AJ 104, 340

Magain P., Surdej J., Swings J.-P., et al., 1988, Nature 334, 325

Michalitsianos A.G., Oliversen R.J., 1995, ApJ 439, 599

Moffat A.F.J., 1969, A&A 3, 455

Reimers D., Köhler T., Wisotzki L., 1996, A&AS 114, 235 Smette A., Robertson J.G., Shaver P.A., Reimers D., Wisotzki L., Köhler T., 1995, A&AS 113, 199

Surdej J., Claeskens J.F., Crampton D., et al., 1993, AJ 105, 2064

Tytler D., Fan X.-M., 1992, ApJS 79, 1

Wisotzki L., Köhler T., Kayser R., Reimers D., 1993, A&A 278, L15

Wisotzki L., Ikonomou M., Köhler T., Reimers D., 1995, A&A 297, L59

Wisotzki L., Groote D., Köhler T., Reimers D., 1996, A&AS 115, 227

This article was processed by the author using Springer-Verlag \LaTeX A&A style file L-AA version 3.